Root cap size and shape influence responses to the physical strength of the growth medium in Arabidopsis thaliana primary roots

Juliette Roue, Hugo Chauvet-Thiry, Nicole Brunel-Michac, François Bizet, Bruno Moulia, Eric Badel, Valerie Legue

Journal of Experimental Botany
doi:10.1093/jxb/erz418 Advance Access Publication 4 November 2019
This paper is available online free of all access charges (see https://academic.oup.com/jxb/pages/openaccess for further details)

RESEARCH PAPER

Root cap size and shape influence responses to the physical strength of the growth medium in *Arabidopsis thaliana* primary roots

J. Roué, H. Chauvet, N. Brunel-Michac, F. Bizet, B. Moulia, E. Badel and V. Legué*

Université Clermont Auvergne, INRA, PIAF, F-63000 Clermont-Ferrand, France

* Correspondence: valerie.legue@uca.fr

Received 2 May 2019; Editorial decision 14 August 2019; Accepted 11 October 2019

Editor: Gwyneth Ingram, CNRS/Ecole Normale Superieure de Lyon, France

Abstract

During the progression of root in soil, root cap cells are the first to encounter obstacles and are known to sense environmental cues, thus making the root cap a potential mechanosensing site. In this study, a two-layered growth medium system was developed in order to study root responses to variations in the physical strength of the medium and the importance of the root cap in the establishment of these responses. Root growth and trajectory of primary roots of Arabidopsis seedlings were investigated using *in vivo* image analysis. After contact with the harder layer of the medium, the root either penetrated it or underwent rapid curvature, thus enabling reorientation of growth. We initially hypothesized that the root-cap structure would affect apex penetration and reorientation, with pointed caps facilitating and domed caps impeding root penetration. This hypothesis was investigated by analysing the responses of Arabidopsis mutants with altered root caps. The primary root of lines of the *fez-2* mutant, which has fewer root-cap cell layers and a more pointed root cap than wild-type roots, showed impaired penetration ability. Conversely, *smb-3* roots, which display a rectangular-shaped cap, showed enhanced penetration abilities. These results, which contradict our original hypothesis, reveal a role for resistance to buckling in determining root penetration abilities.

Keywords: Curvature, medium strength, Phytagel medium, root biomechanics, root buckling, root cap, root growth.

Introduction

Roots grow in a complex soil environment that exhibits spatial and temporal heterogeneities, for example arising from the presence of sand particles, stones, or areas of hardpan. The ability of roots to penetrate the soil and to overcome physical obstacles depends either on their ability to find a path of least resistance, or on their ability to generate sufficient force to go through the obstacle (Bengough *et al.*, 2010; Vollsnes *et al.*, 2010; Colombi *et al.*, 2017*a*). The force needed to penetrate soil, which is provided by root growth, is determined by the soil strength. In natural conditions, soil strength—commonly estimated by penetrometer measurements—is of the order of 1 MPa and may increase as the result of soil compaction or soil drying (Jin *et al.*, 2013; Kolb *et al.*, 2017).

In a few laboratory studies, changes in soil strength have been mimicked using simplified models such as two-layer Phytagel-based growth media, in which the layers contain different concentrations of Phytagel (Yamamoto *et al.*, 2008; Yan *et al.*, 2017). It has been shown that adjusting the concentration modulates the physical strength of the growth medium (Schiavi *et al.*, 2016). In such experiments where roots are consecutively faced with a compliant and a stiff layer, the tips are submitted to increasing axial stress. Roots that do not manage to generate

sufficient force to penetrate the lower layer undergo buckling, which dramatically changes the growth trajectory and the straightness of the root (Massa and Gilroy, 2003; Silverberg *et al.*, 2012; Bizet *et al.*, 2016). The maximal axial force that a root is able to apply before buckling, given by Euler's law, depends on the rigidity, the length of the growth zone, and the diameter of the root to the power of four (Timoshenko and Goodier, 1970). In accordance with Euler's law, species with a greater increase in root diameter in response to the strength of the medium are more efficient in penetrating strong layers (Materechera *et al.*, 1992). The shape of the root tip is also an important feature that modulates the responses to the strength of the medium (Ruiz *et al.*, 2016; Colombi *et al.*, 2017*b*). In compacted soils, root tips with an acute opening angle grow faster than root tips with a blunted geometry (Iijima *et al.*, 2003*a*, 2003*b*; Colombi *et al.*, 2017*b*). Colombi *et al.* (2017*b*) showed that the shape of the tip influences the penetration stress experienced by roots by modulating the distribution of the local compaction concentrated around the tip.

The shape of the root tip arises from the shape of the cap that covers and protects the root apical meristem. In Arabidopsis, the root cap is organized in 3–5 cell layers of increasing age, and is composed of the columella (COL) and the lateral root cap (LRC) (Arnaud *et al.*, 2010; Kumpf and Nowack, 2015). Every formative division of root-cap stem cells generates a new differentiating cell layer that pushes the older layers towards the root periphery. COL mature cells are known to sense gravity whereas LRC mature cells principally act as secretory cells (Kumpf and Nowack, 2015; Sato *et al.*, 2015). At the periphery of the root cap, LRC mature cells undergo programmed cell death (PCD) and are degraded on the root surface in the elongation zone whereas COL mature cells are sloughed off, releasing border-like cells into the rhizosphere (Vicré *et al.*, 2005; Fendrych *et al.*, 2014). The balance between cell production and cell sloughing controls the changes in root-tip size and shape (Barlow, 2003). The study of root-cap formation has resulted in the identification of the molecular factors involved in cell production, differentiation, and sloughing. Among these, the FEZ and SOMBRERO (SMB) transcription factors from the NAC family (NO APICAL MERISTEM, *ARABIDOPSIS* TRANSCRIPTION ACTIVATION FACTOR, CUP-SHAPED COTYLEDON) have been identified. FEZ specifically promotes periclinal divisions of COL and LRC stem cells (Willemsen *et al.*, 2008). The *fez-2* loss-of-function mutant exhibits a lower rate of periclinal division of the root-cap stem cells, which leads to a reduction of COL and LRC cell layers compared to wild-type roots (Willemsen *et al.*, 2008; Bennett *et al.*, 2014). SMB prevents the division of the differentiating root-cap daughter cells and promotes their differentiation. Additional COL and LRC cell layers are observed in the *smb-3* loss-of-function mutant (Willemsen *et al.*, 2008; Bennett *et al.*, 2010). Moreover, SMB seems to indirectly regulate the PCD of LRC mature cells by targeting PCD- and cell clearance-specific genes (Fendrych *et al.*, 2014; Huysmans *et al.*, 2018). In the *smb-3* mutant, LRC cell death is delayed, causing an increase in LRC size so that it reaches into the elongation zone. After cell death, unprocessed dead cells accumulate on the *smb-3* root surface (Fendrych *et al.*, 2014).

The objective of this study was to investigate the role of the structure of the root cap in the establishment of root responses to the physical strength of the growing medium. We hypothesized that pointed caps would facilitate root penetration whilst domed caps would make penetration harder. We studied the root responses of the *fez-2* and *smb-3* Arabidopsis mutant lines because of their contrasting cap structure. We characterized the cap morphology of the roots in order to determine whether the loss or gain of cell layers affected root-cap size and shape. Col-0, *fez-2*, and *smb-3* roots were then grown in two-layer Phytagel media of increasing mechanical resistance. Using a spatio-temporal analysis, we characterized the ability of the roots to penetrate the harder medium, the root growth rate, and the root curvature. We found that penetration ability and the reorientation in *fez-2* and *smb-3* primary roots were affected in the opposite way to how we had hypothesized.

Material and methods

Plant material and growth conditions

The wild-type strain of *Arabidopsis thaliana* (Col-0) and the *fez-2* and *smb-3* null-mutants used for the experiments were provided by the laboratory of B. Scheres (University of Utrecht, The Netherlands; Willemsen *et al.*, 2008; Bennett *et al.*, 2010, 2014). For all the experiments, Phytagel-based growth media were developed. The growth medium consisted of half-strength Murashige and Skoog (MS/2) medium adjusted to pH 5.7 and containing Phytagel at different concentrations. Two-layer media were made of an upper layer of medium containing 0.2% (w/v) Phytagel and a lower layer containing 0.2%, 0.3%, or 0.5 % Phytagel (Supplementary Fig. S1 at *JXB* online), hereafter referred to as 0.2/0.2, 0.2/0.3 and 0.2/0.5 medium. The two-layer media were poured into specific culture chambers that consisted of polycarbonate boxes measuring 100×20 mm and 60 mm deep, which enabled roots to grow vertically inside the growth medium. The two-layer media were prepared as follows. Sterilized MS/2 medium containing 0.2%, 0.3%, or 0.5% Phytagel was poured under aseptic conditions into the culture chambers to a height of 30 mm. After 10 min, sterilized MS/2 medium containing 0.2% Phytagel was poured onto the lower layer to a height of 10 mm.

Arabidopsis seeds were surface-sterilized for 10 min with 30% (v/v) sodium hypochlorite solution added to 2% (v/v) Triton X-100. After five washes in sterile distilled water, 10 seeds were gently placed on the surface of the growth medium. The culture chambers were sealed, kept at 4 °C in the dark for 2 d, and then placed at 23 °C under a 16-h photoperiod.

Mechanical properties of Phytagel growth medium

We performed compressive and penetration tests on the Phytagel media to determine their elastic modulus and mechanical penetration resistance.

Measurement of elastic modulus

Growth media containing 0.2–1.2% (w/v) of Phytagel were poured into 10-mm deep Petri dishes. Then, 20×20×10 mm^3 samples were cut and placed in a universal testing device (Instron 5565). A uniaxial compressive load was applied on the surface of the gel by displacement of the upper plate with a constant loading rate of 0.5 mm min^{-1} (Fig. 1A). A 100-N load cell recorded the force needed to deform the samples. After a typical contact step, the loading force increased with the compression of the sample before decreasing notably when the sample slipped or ruptured. Real-time load and displacement recordings provided characteristic mechanical stress–strain curves (Fig. 1B). In the linear portion of the curve, i.e. when stress is proportional to strain, deformation is considered to be elastic (Schiavi *et al.*, 2016) and the value of the elastic modulus (E) of the Phytagel samples was determined from the ratio between the

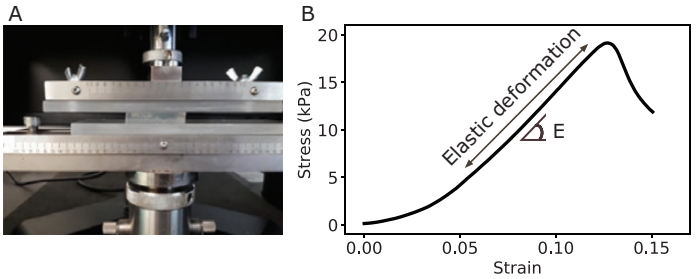

Fig. 1. Instrument used for compressive tests and an example of a characteristic stress–strain curve obtained. (A) A 1.2% Phytagel cube placed in an Instron device and compressed by an upper plate at a loading rate of 0.5 mm min^{-1}. (B) Typical stress–strain curve resulting from the compressive test. The elastic modulus, *E*, corresponds to the slope of the linear portion of the curve, which is the zone of elastic deformation. (This figure is available in colour at *JXB* online.)

incremental stress $\Delta\sigma$ and the incremental strain rate $\Delta\varepsilon$ according to Hooke's law:

$$E = \Delta\sigma/\Delta\varepsilon \quad (1)$$

where

$$\sigma = F/A \quad (2)$$

$$\varepsilon = \frac{\Delta l}{l_0} \quad (3)$$

and F is the compression force (N), A is the surface area of the cross-section of the sample (m^2) on which the force is applied, l_0 is the initial thickness of the sample (m), and Δl is the change in thickness, i.e. the displacement of the plate (m). Compressive tests were repeated for three samples of each Phytagel concentration.

Measurement of resistance to penetration

Penetration tests were conducted for the 0.2/0.2, 0.2/0.3, and 0.2/0.5 two-layer media using Phytagel medium samples that were prepared in the same culture chambers as used for root growth. A 2.5-mm diameter needle was attached to a load cell (Instron, 100 N max) and moved downward into the gel at a rate of 1 mm min^{-1}. Real-time recording of the force-displacement curve enabled the determination of the maximal force required for the rupture of the interface between the upper and the lower layer.

Root-cap shape and determination of sharpness index

Col-0, *fez-2*, and *smb-3* lines were grown in a 0.2% single-layer medium and at 5 d old primary roots were extracted and placed on a microscope slide. The roots were stained with 10 µg ml^{-1} propidium iodide (PI, Sigma Aldrich) and observed using a LSM 800 laser-scanning microscope (Zeiss) coupled to an Apochromat X20 lens.

To characterize the root-cap size and shape of each genotype, the length of the vertical section, L_R, the diameter of the root at the quiescent centre, D_R, and the area of the radial section of the root cap, A_R, were measured in longitudinal sections of the medium using the ImageJ software (Schneider *et al.*, 2017) (Fig. 2). An *inverse* Sharpness Index (*i*SI) of the root cap was calculated according to the following equation:

$$i\mathrm{SI} = \frac{A_R - (L_R D_R)/2}{L_R D_R/2} \quad (4)$$

The closer *i*SI is to 0, the more the root cap is pointed. Conversely, the closer *SI* is to 1, the more the root cap has a rectangular shape.

Length of the root growth zone

Col-0, *fez-2*, and *smb-3* lines were grown in a 0.2% single-layer medium and at 5 d old primary roots were gently extracted and stained with

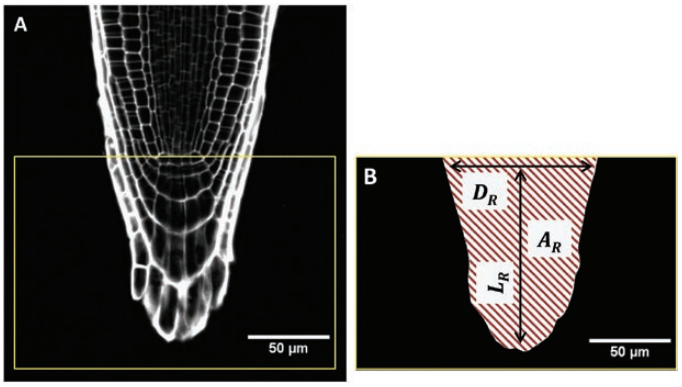

Fig. 2. Characterization of the size and shape of the root cap in Arabidopsis. (A) Confocal microscope image of a 5-d-old root of Col-0 stained with propidium iodide. The box indicates the section of the root cap for which the size and shape were measured. (B) Root cap section threshold using the Image J software. The morphology of the root cap was characterized by its length, L_R (from the quiescent centre, QC, to the tip of the cap), the diameter of the root at the QC, D_R, and the area of the root tip section, A_R (corresponding to the hatched area). These three measures enabled calculation of the *inverse* Sharpness Index (eqn 4). (This figure is available in colour at *JXB* online.)

10 µg ml^{-1} PI. Using confocal optical sections of the roots, the length of the cortical cells was measured from the quiescent centre up to 2 mm. Assuming the roots were in a steady state with a constant cell flux, the local velocity over the root apex (i.e. the rate at which a cell moves away from the quiescent centre) was calculated from the cell length measurements (for details see Silk and Erickson, 1979; Silk, 1992; Liu *et al.*, 2013). The velocity profile was used to calculate the length of the growth zone of the roots, which corresponded to the length of the root section from the quiescent centre to the point where the velocity reached 94% of the maximal value (Supplementary Fig. S2).

Maximal root growth forces

The maximal axial force the roots were able to apply on the two-layer medium interface before reorientation of the root apex was estimated for Col-0, *fez-2*, and *smb-3* roots grown in 0.2/0.3 medium. After contact between the root and the interface, root axial growth induced a deflection of this interface until the root curved or the root apex deviated. The shape of the interface just before root apex reorientation was traced using ImageJ software and the maximal deflection, d, of the interface was measured with regards to its initial position (i.e. before contact with the root). The shape of the tip of the root cap was fitted by a circle of radius R. The maximal force before root reorientation, F_{crit}, applied on the interface by the root apex was then estimated using the theory of elastic contact between a sphere and a half-space medium (Hanaor *et al.*, 2015):

$$\boldsymbol{F_{crit}} = \frac{4}{3}\boldsymbol{E^*}\boldsymbol{R}^{\frac{1}{2}}\boldsymbol{d}^{\frac{3}{2}} \quad (5)$$

where

$$\frac{1}{\boldsymbol{E^*}} = \frac{1-\boldsymbol{\nu}_1^2}{\boldsymbol{E}_1} + \frac{1-\boldsymbol{\nu}_2^2}{\boldsymbol{E}_2} \quad (6)$$

and E_1 and E_2 are the elastic moduli of the lower medium layer and of the root apex, respectively, and ν_1 and ν_2 are the Poisson ratios of the lower layer and the root apex, respectively. Assuming that E_2 was much larger than E_1, the second part of the equation was neglected, and the value of ν_1 was estimated as 0.5 (Ahearne *et al.*, 2005).

Time-lapse photography and image processing

Root growth and orientation were subjected to time-lapse imaging from 5 d after sowing. Two Nikon D7100 cameras equipped with macro

lenses (AF-S micro NIKKOR 60mm f/2.8G ED) and controlled by DigiCamControl software were placed on a rack in front of the culture chambers. Images of the roots growing in the two-layer media were recorded every 5 min for at least 24 h. Only the roots remaining in the focal plane of the objectives were analysed. All images were pre-treated using the Rawtherapee software (v4.2.1; https://rawtherapee.com/) and were analysed using the RootStem Extractor software developed by the PIAF laboratory (Chauvet *et al.*, 2016). Briefly, the software enabled extraction of the topological skeleton of each root by screening the pictures perpendicularly to the root axis with a step of 0.3 pixels. The length of the root on each picture and the local inclination as a function of the curvilinear abscissa can be computed from the coordinates of the skeleton. The root length as a function of time enabled us to calculate root growth rate by linear fit. Curvature intensity along the root was obtained by deriving the local inclination as a function of time and space. The curvature intensity data are presented in graphs composed of three dimensions: a vertical axis corresponding to root length from the beginning of the measurement, a horizontal axis corresponding to time, and a colour bar that depicts curvature intensity. On the spatio-temporal graphs, the green colour indicates a straight section of the root, while the red and blue colours depict the highest positive and negative curvatures, respectively.

Gravitropic responses of the roots

Col-0, *fez-2*, and *smb-3* roots were grown vertically into a 0.5% Phytagel single-layer medium for 5 d. The culture chambers were tilted by 90° (i.e. horizontal) and images of the primary roots were then recorded every 10 min for 22 h. Analysis of the time-lapse images with RootStem Extractor was used to measure root length and root-tip angle over time (Supplementary Fig. S3). These data were used to calculate the gravitropic response by applying the equation described by Chauvet *et al.* (2016).

Statistical analysis

All data were analysed using R software (RStudio, R.3.3.4; www.rstudio.com) and are presented as means (±SD) in the Results. The Shapiro–Wilk test was used to test for normal distribution of the data and the Bartlett test was used to test for homoscedasticity. One- or two-way ANOVA were used to determine whether the effect of each factor was significant. When significant differences were observed, post-hoc analyses based on Tukey's test were applied to the data.

Results

Phytagel concentration affects both the rigidity and penetration resistance of the growth medium

The elastic modulus, E, obtained from compressive tests, was measured for Phytagel concentrations ranging from 0.2–1.2% (Fig. 3A, B). The 0.2%, 0.3%, 0.5%, and 1.2% media had mean (±SD) E values of 3.1±0.2 kPa, 7.6±1.4 kPa, 31.9±6.6 kPa, and 158.3±18.3 kPa, respectively (Fig. 3B), indicating that E was highly dependent on the Phytagel concentration.

Penetrometer tests were performed in 0.2/0.2, 0.2/0.3, and 0.2/0.5 two-layer media (Fig. 3C, D). The curves of the compression force versus needle displacement were divided into two steps: (I) after the first contact with the lower layer surface, the compression force increased markedly until reaching a maximal value; and (II) as the needle penetrated the lower layer, the loading force rapidly collapsed (Fig. 3C). The specific pattern of the displacement-force curves illustrated the presence of the interface between the two medium layers, the rupture of which required a specific force, called the maximal strength, which may have reflected a slight drying out of the surface of the lower layer during the 10 min preceding the pouring of the upper layer. The maximal strength was 0.03±0.01 N in the 0.2/0.2 medium, 0.05±0.02 N in the 0.2/0.3 medium, and 0.11±0.02 N in the 0.2/0.5 medium (Fig. 3D). Thus, the maximal strength increased significantly with the Phytagel concentration of the lower medium layer.

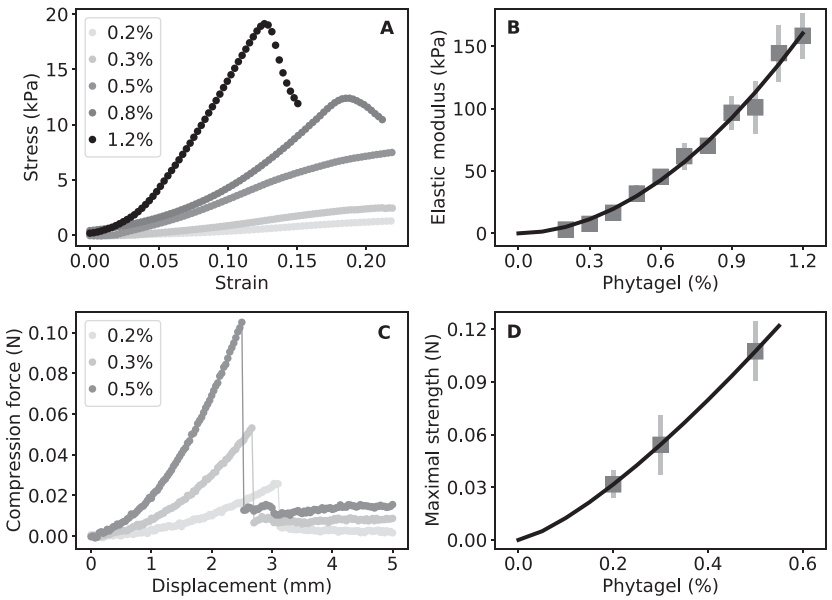

Fig. 3. Mechanical properties of Phytagel growth media. (A) Stress–strain curves resulting from compressive tests performed on cubes of growth medium containing Phytagel at concentrations ranging from 0.2–1.2%. The data shown correspond to individual measurements. (B) The elastic modulus, E, was estimated using the slope of the linear portion of the stress–strain curve (Fig. 1). Data are means (±SD), n=3. (C, D) Penetrometer tests performed to examine the mechanical resistance of the interface in two-layer media. (C) Compression force during penetration of the needle into the lower layer of medium of 0.2%, 0.3%, and 0.5% Phytagel. The reference starting point for displacement corresponds to the first contact between the needle tip and the interface. The data shown correspond to individual measurements. (D) Maximum strength required for the needle to induce rupture of the interface as a function of the Phytagel concentration of the lower layer of the medium. Data are means (±SD), n=4.

The Arabidopsis fez-2 *and* smb-3 *mutations affect root-cap size and shape in primary roots*

Several morphological traits were examined in the Col-0, *fez-2*, and *smb-3* primary roots in order to specify the impact of the mutations on root-cap size and shape (Fig. 4). Compared to the wild-type (WT), the *fez-2* root cap was shorter and narrower at the base, whereas the *smb-3* cap was longer and larger at the base (Fig. 4D, E). However, mean root diameter measured at 500 μm from the tip of the cap was not significantly different between the three genotypes (Supplementary Fig. S4). Estimation of the *inverse* Sharpness Index indicated that *fez-2* root caps (*i*SI=0.30±0.07) were significantly more pointed than WT caps (0.41±0.06) whilst *smb-3* displayed a more rectangular shape (0.5±0.13; Fig. 4F). Our morphological characterizations thus showed that *fez-2* and *smb-3* mutations altered the root cap size and shape in Arabidopsis primary roots.

The smb-3 *mutation affects root growth and the gravitropic response whereas the* fez-2 *mutation does not*

From a kinematic analysis, the mean length of the growth zone from the quiescent centre to the end of the elongation zone was estimated to be 917±194, 846±303, and 898±299 μm in the WT, *fez-2*, and *smb-3* lines, respectively (Fig. 5A, Supplementary Fig. S2), suggesting that the mutations may not affect the size of the zone. Analysis of root growth in a 0.2% Phytagel single-layer medium showed that the mean growth rate of WT (3.2±0.8 μm min^{-1}) and *fez-2* (3.0±0.7 μm min^{-1}) roots was not significantly different, whereas *smb-3* roots grew more slowly (1.6±0.3 μm min^{-1}) (Fig. 5B). Moreover, WT and *fez-2* roots exhibited a similar gravitropic response (0.17±0.05 and 0.17±0.02, respectively), whereas *smb-3* roots exhibited a significantly higher response (0.36±0.15; Fig. 5C, Supplementary Fig. S3). Our preliminary studies thus showed that the *fez-2* mutation mainly affects the size and shape of the root cap whereas the *smb-3* mutation also affects the root growth and gravitropic responses.

The fez-2 *and* smb-3 *mutations affect the ability of primary roots to penetrate the harder layer of the growth medium*

In order to understand the role of cap structure in the root response to an increase in the strength of the growth medium, the penetration abilities of the primary roots of the three genotypes were compared in two-layer Phytagel media. In the 0.2/0.2 medium, where the increase in strength was the weakest, 100% of the WT and *smb-3* roots crossed the interface to penetrate the lower layer, whereas only 83% of the *fez-2* roots were able to do so (Table 1). In the 0.2/0.3 medium, 60% of the WT primary roots penetrated the 0.3% lower layer whilst 80% of the *smb-3* and 28% of the *fez-2* roots were able to do so. Finally, only 1.7 % of the WT roots and 18.3% of the *smb-3* roots penetrated the 0.5% lower layer in the 0.2/0.5 medium, and none of the *fez-2* roots were able to do so.

Thus, compared with the WT, the *fez-2* roots exhibited impaired penetration ability in response to an increase in the strength of the growth medium, whereas the *smb-3* roots exhibited enhanced penetration ability. In order to determine the cause of these differences, we estimated the critical force that each root was able to apply on the two-layer medium interface before apex reorientation occurred.

The critical axial growth force of primary roots is impaired in fez-2 *and enhanced in* smb-3

The critical axial force was estimated for primary roots of the three genotypes growing in the 0.2/0.3 medium, in which

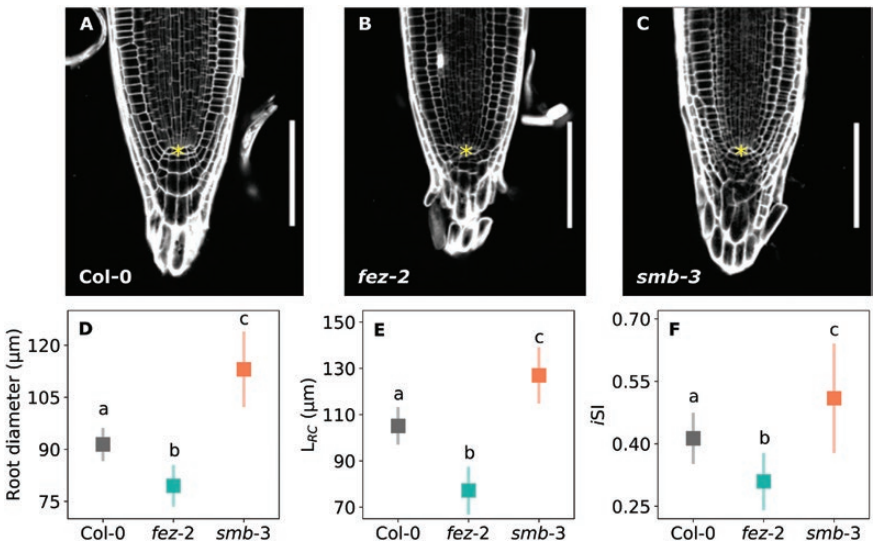

Fig. 4. Morphology of Arabidopsis Col-0, *fez-2*, and *smb-3* root caps. (A–C) Representative confocal microscope images of 5-d-old roots that were grown in compliant medium containing 0.2% Phytagel. The roots are stained with propidium iodide. Asterisks indicate the quiescent centre (QC). The scale bar is 100 μm. (D) Diameter of the roots at the QC. (E) Length of the root cap from the QC to the tip of the root cap, L_R (Fig. 2). (F) The *inverse* Sharpness Index (*i*SI) of the root tips (eqn 4). Data are means (±SD), *n*=20. Different letters indicate significant differences as determined using one-way ANOVA followed by Tukey's test ($P<0.05$).

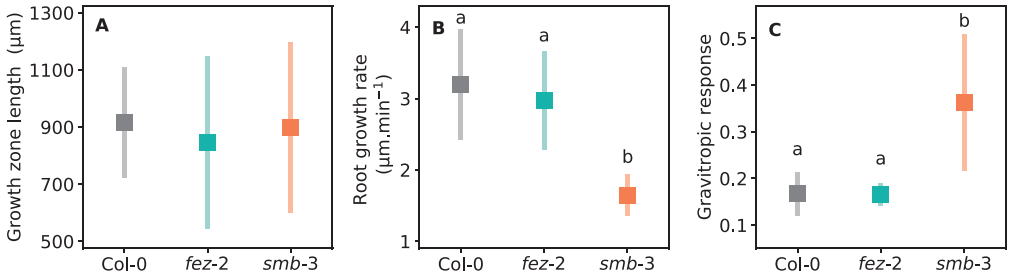

Fig. 5. Growth and gravitropic responses of Arabidopsis Col-0, *fez-2*, and *smb-3* root apexes. (A) Length of the growth zone from the quiescent centre to the end of the elongation zone, estimated using a kinematic analysis. (B) Growth rates of roots growing in compliant 0.2% Phytagel single-layer medium. (C) Gravitropic response of roots after tilting by 90°. The data are expressed in dimensionless units (Chauvet *et al.* (2016). Data are means (±SD), $14 \leq n \leq 18$ (A), $n=15$ (B), and $14 \leq n \leq 16$ (C). Different letters indicate significant differences as determined using one-way ANOVA followed by Tukey's test ($P<0.05$).

Table 1. *Penetration ability of Arabidopsis Col-0,* fez-2, *and* smb-3 *primary roots in two-layer Phytagel media*

Genotype	Penetrating roots (%)		
	0.2/0.2 interface	0.2/0.3 interface	0.2/0.5 interface
Col-0	100.00±0.00 [a]	60.00±3.65 [c]	1.67±1.67 [e]
fez-2	83.33±4.94 [b]	28.33±3.07 [d]	0.00±0.00 [e]
smb-3	100.00±0.00 [a]	80.00±5.16 [b]	18.33±4.77 [d]

Penetration ability is represented by the percentage of roots that were able to penetrate the 0.2%, 0.3%, and 0.5% lower layers of the Phytagel media. The upper layer was 0.2% in each case. For each genotype and interface, 10 roots in each of six replicate preparations of growth medium were observed 8 d after germination, and the data are presented as means (±SD), $n=60$. Different letters show significant differences as determined using two-way ANOVA followed by Tukey's test ($P<0.05$).

the greatest differences in penetration ratio were observed between the three lines (Table 1). Upon contact, root axial growth induced a deflection of the interface until either the interface ruptured or a zone of curvature in the root was initiated. We measured the deflection of the interface before curvature initiation for roots that did not penetrate the lower layer (Fig. 6A). Wild-type roots displaced the interface to a mean maximal depth, d, of 0.37±0.03 mm, whilst for *fez-2* roots d=0.27±0.01 mm and for *smb-3* roots d=0.49±0.03 mm (Fig. 6B). The values of d together with the radius of the tip of the root cap and the rigidity of the lower layer of the medium (E=7.6 kPa) made it possible to estimate the critical axial growth force of the primary roots (Fig. 6C), which were found to be 1.12±0.14 10^{-3} N for the WT, 0.66±0.07 10^{-3} N for *fez-2*, and 1.77±0.18 10^{-3} N for *smb-3*. This confirmed that *smb-3* roots were able to apply a higher axial force on the interface compared with then WT, whilst *fez-2* roots applied a weaker force.

The fez-2 *and* smb-3 *roots exhibit altered patterns of curvature in response to an increase in the strength of the growth medium*

Roots that did not apply a sufficient axial force to induce rupture of the interface between the two layers of media reorientated their growth as the result of initiation of zones of curvature. This initiation was monitored as a function of the increase in the strength of the medium and as a function of the genotype (Supplementary Videos S1–S7). Representative examples of WT, *fez-2*, and *smb-3* roots reorientating their growth in 0.2/0.3 and 0.2/0.5 media are presented in Figs 7–9.

Following contact with the 0.3% interface, non-penetrating roots first grew downwards against the interface and deformed it until a first zone of curvature was formed (Fig. 7). This first zone appeared at 515±98, 603±33, and 398±53 µm from the tip of the root cap in WT, *fez-2*, and *smb-3* roots, respectively. Once established, the curvature covered a zone of 657±121, 977±58, and 414±73 µm in WT, *fez-2*, and *smb-3* roots, respectively (Fig. 7, Supplementary Table S1). The length of the zone was significantly greater in *fez-2* roots than in *smb-3* roots, but no significant differences were observed between the WT and mutant roots. Initiation of the first zone of curvature induced lateral deviation of the *fez-2* root apex whereas the WT and *smb-3* apexes continued to grow downwards. These different behaviours led to the establishment of two distinct root shapes (Fig. 8, Supplementary Videos S1–3). In WT and *smb-3* roots, several similar zones of curvature were initiated successively, leading to the formation of one or more curls (Fig. 8A, Supplementary Videos S1, S2); thus, these roots developed a 'curly' shape in the 0.2/0.3 medium. In *fez-2* roots, the lateral deviation of the apex was followed by the initiation of a second zone of curvature with characteristics distinct from the first zone (Figs 7B2, 8B). Whereas the first zone was maintained after its establishment, the second one moved and kept a constant distance from the tip of the root cap (Fig. 7). The establishment of the two distinct zones of curvature in *fez-2* roots led to the formation of a 'step-like' shape (Fig. 8B).

In the 0.2/0.5 medium, all the WT and *fez-2* roots developed a step-like shape following contact with the interface (Fig. 9, Supplementary Videos S4, S5). For the *smb-3* line, three distinct root shapes were observed: 'curly', 'wavy', and 'step-like' shapes (Supplementary Videos S6, S7). The spatio-temporal establishment of the step-like shape of primary roots was compared between the three genotypes. After contact with the 0.2/0.5 interface, a first zone of curvature was formed at 540±50, 664±64, and 407±32 µm from the tip of the cap in WT, *fez-2*, and *smb-3* roots, respectively (Fig. 9). In *fez-2* roots, curvature was initiated significantly further from the tip than in *smb-3* roots, but no significant differences were observed between the WT and the mutant roots (Supplementary Table S2). Once

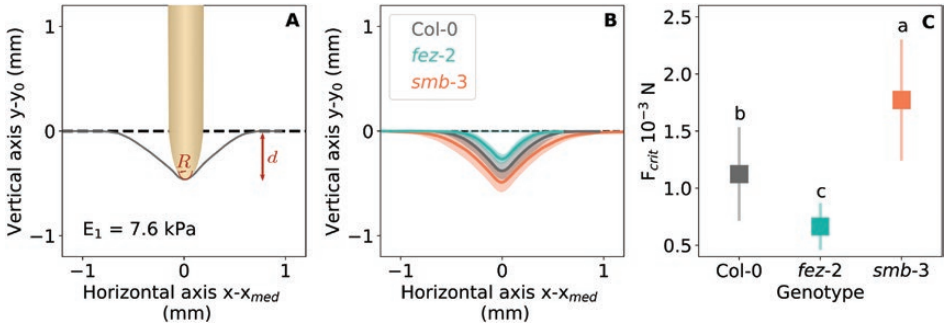

Fig. 6. Critical axial force of Arabidopsis Col-0, *fez-2*, and *smb-3* roots. (A) Schematic diagram of a root apex growing against the 0.2/0.3 % Phytagel interface with elastic modulus E_1=7.6 kPa. The curve represents the shape of the interface just before initiation of root curvature: *d* is the corresponding maximal deflection of the interface and *R* is the radius of the root tip in contact with the surface. The dashed line corresponds to the initial shape of the interface before contact with the root apex. (B) The shapes of the interface (*E*=7.6 kPa) as deformed by the root tips of the three genotypes just before initiation of curvature. The solid lines are means of *n*=10 replicates and the shading represents ±SD. The dashed line corresponds to the initial shape of the interface before contact with the root apex. (C) Evaluation of the critical force, F_{crit}, that the roots were able to apply on the interface before reorientating (eqn 5). Data are means (±SD), *n*=10.. Different letters indicate significant differences as determined using one-way ANOVA followed by Tukey test's (*P*<0.05).

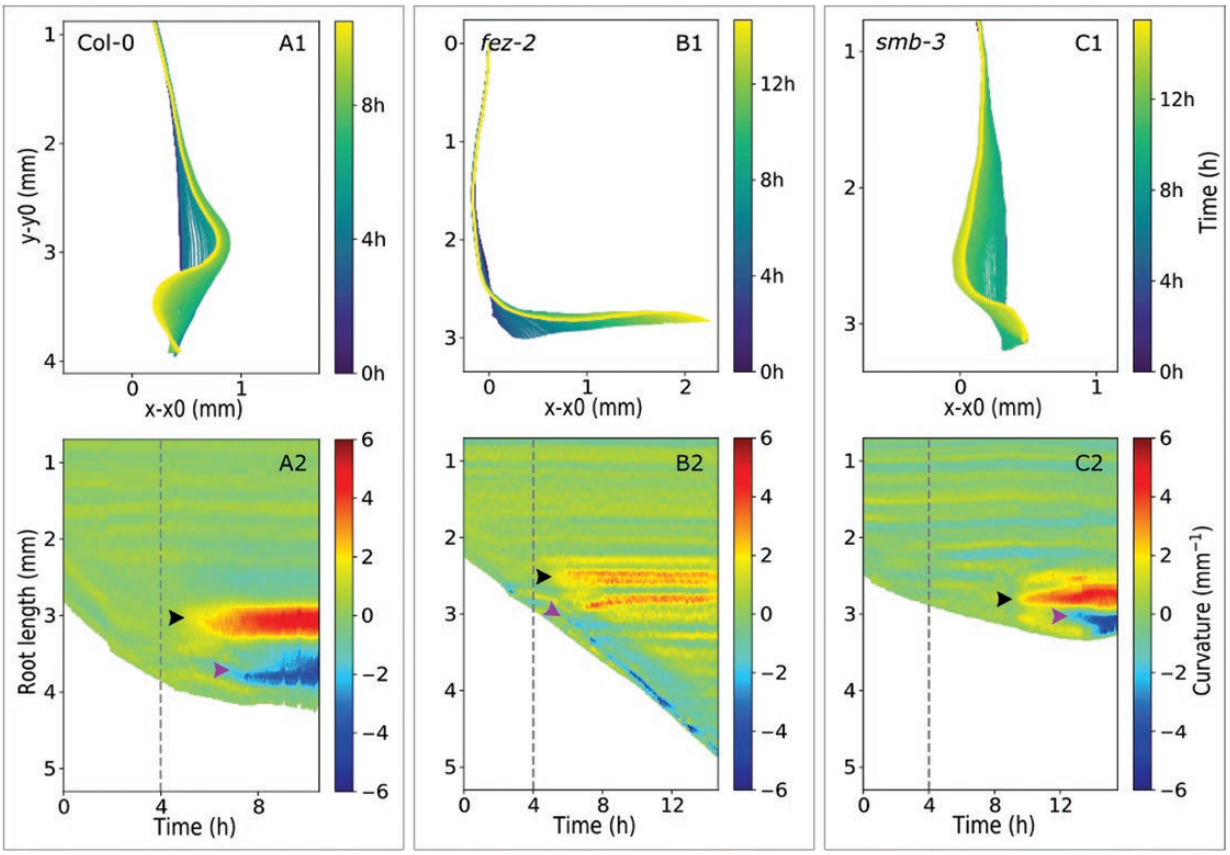

Fig. 7. Spatio-temporal characterization of apex reorientation of Arabidopsis Col-0, *fez-2*, and *smb-3* roots in the 0.2/0.3 % Phytagel medium. (A1, B1, C1) Skeleton and (A2, B2, C2) spatio-temporal analyses of primary roots reorientating after contact with the 0.2/0.3 interface for (A) Col-0, (B) *fez-2*, and (C) *smb-3*. In the spatio-temporal graphs, root length is presented as a function of time and the colours represent curvature intensity: negative for right-handed curvature and positive for left-handed curvature. Green corresponds to the straight zones of the roots, while red and blue depict the highest positive and negative curvatures, respectively. The dashed lines indicate the time of initial contact between the root apex and the interface. The black and purple arrowheads indicate the initiation of the first and the second zones of curvature, respectively.

established, the curvature extended over a zone of 657±121, 977±58, and 414±73 μm in the WT, *fez-2*, and *smb-3* roots, respectively (Fig. 9). Thus, the zone of curvature was significantly longer in *fez-2* roots than in WT and *smb-3* roots. Moreover, the maximal curvature intensity was significantly weaker in *fez-2* roots (2.3±0.5 mm^{-1}) than in WT (4.7±0.5 mm^{-1}) and *smb-3* roots (4.8±0.6 mm^{-1}). As the apex reorientated its growth, the roots of all three genotypes showed a second zone of curvature, the establishment of which showed common characteristics except for the maximal intensity, which was significantly weaker in *fez-2* roots (Fig. 9, Supplementary Table S2). The second zone of curvature remained at a constant

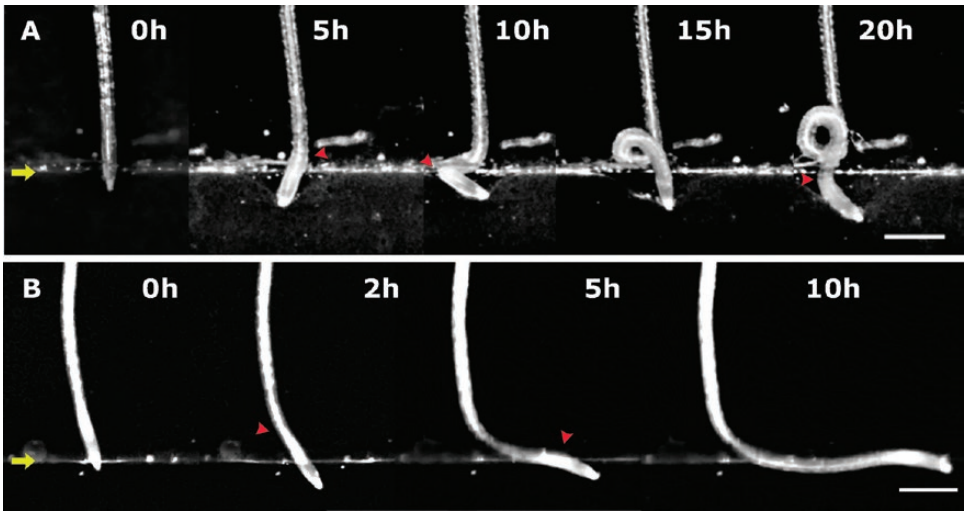

Fig. 8. Major time-steps in the establishment of the curly (A) and step-like (B) root morphologies after contact between the Arabidopsis root apex and the interface of the 0.2/0.3 % Phytagel medium. Representative images are shown of root apex reorientation and curvature of roots that did not penetrate the lower layer in the 0.2/0.3 medium at 0–20 h after contact with the interface. (A) A wild-type (Col-0) root that developed a characteristic curly morphology. (B) A *fez-2* root that developed a characteristic step-like morphology. The yellow arrows indicate the 0.2/0.3 interface. Red arrowheads indicate the formation of zones of curvature. to the scale bars are 500 μm.

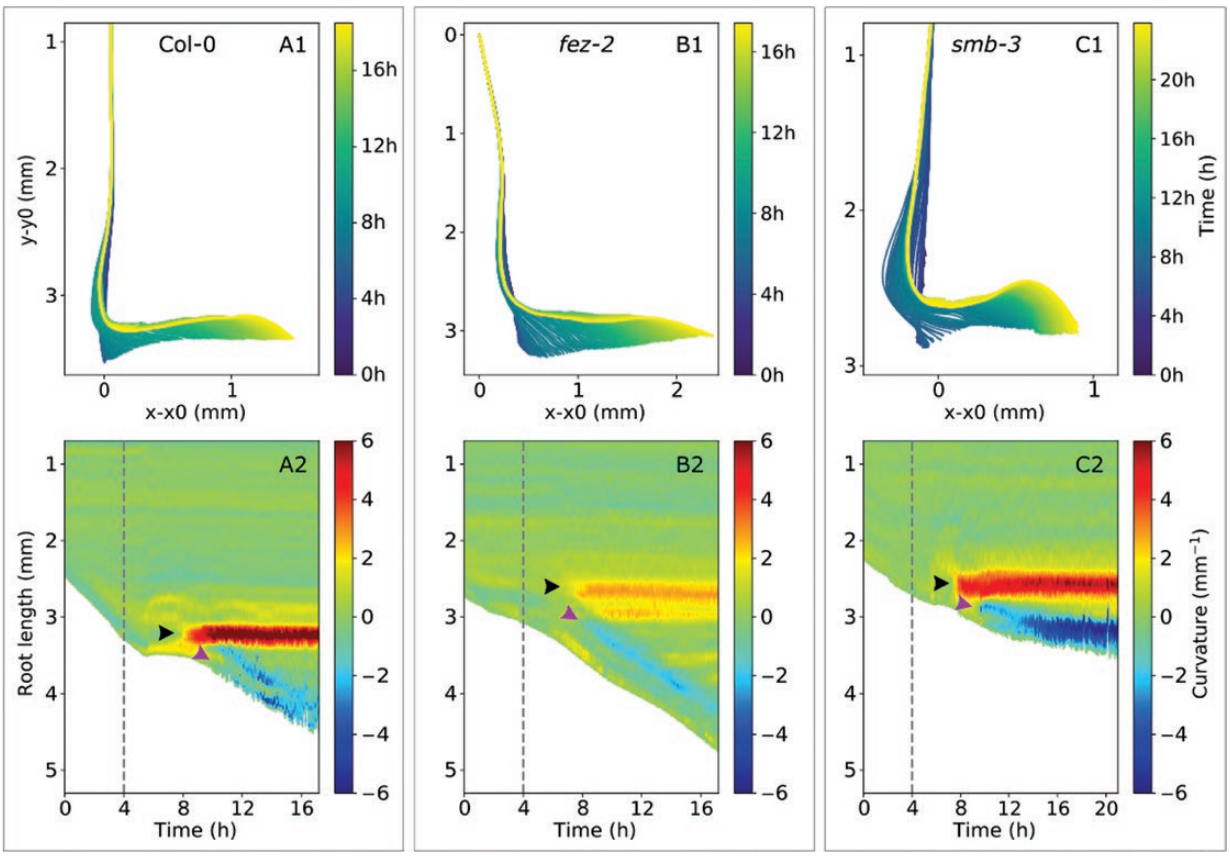

Fig. 9. Spatio-temporal characterization of apex reorientation of Arabidopsis Col-0, *fez-2*, and *smb-3* roots in the 0.2/0.5 % Phytagel medium. (A1, B1, C1) Skeleton and (A2, B2, C2) spatio-temporal analyses of primary roots reorientating after contact with the 0.2/0.5 interface for (A) Col-0, (B) *fez-2*, and (C) *smb-3*. In the spatio-temporal graphs, root length is presented as a function of time and the colours represent curvature intensity: negative for right-handed curvature and positive for left-handed curvature. Green corresponds to the straight zones of the roots, while red and blue depict the highest positive and negative curvatures, respectively. The dashed lines indicate the time of initial contact between the root tip and the interface. The black and purple arrowheads indicate the initiation of the first and the second zones of curvature, respectively.

distance from the tip of the cap during root growth along the 0.2/0.5 interface.

These two-layer media experiments demonstrated that root apex reorientation and the establishment of zones of curvature

were affected by both the mechanical resistance of the interface and by the size and shape of the root cap.

Root growth rates in the three genotypes respond differently to increases in the strength of the medium

Growth rates were determined for WT, Col-0, *fez-2*, and *smb-3* roots in media with Phytagel interfaces of 0.2/0.2, 0.2/0.3, and 0.2/0.5.

In the 0.2/0.2 medium only the growth rates of penetrating roots were measured, whilst in the 0.2/0.3 medium the growth rates were measured for both penetrating and reorientating roots (Supplementary Tables S3, S4). In wild- reorientating roots of the WT, the contact between the root and the interface was followed by a significant 60% decrease in mean growth rate (Fig. 10A). Unfortunately, our experimental system based on 2D visualization of the roots prevented measurement of the root growth rate through to the end of the reorientation of the apex. A significant 60% decrease in mean root growth rate was also observed in reorientating roots of *smb-3* whereas no significant decrease was observed in reorientating roots of *fez-2* (Fig. 10A, Supplementary Table S4).

In the 0.2/0.5 medium, the growth rate of WT roots decreased by 37% after contact with the interface (upper layer 3.0±0.2 μm min^{-1}, lower layer 1.9±0.3 μm min^{-1}; Fig. 10B), and the initial growth rate did not recover when reorientation of the apex was complete. The reorientation of the apex of *smb-3* roots after contact with the interface was also accompanied by a significant 44% decrease in mean growth rate (Fig. 10B, Supplementary Table S4). In contrast, *fez-2* roots showed no variation in growth rate after contact with the interface.

These results showed that the increase in the strength of the medium in the two-layer system affected the growth rate of WT roots, and this effect seemed to be altered in the roots of the mutants, especially for *fez-2*.

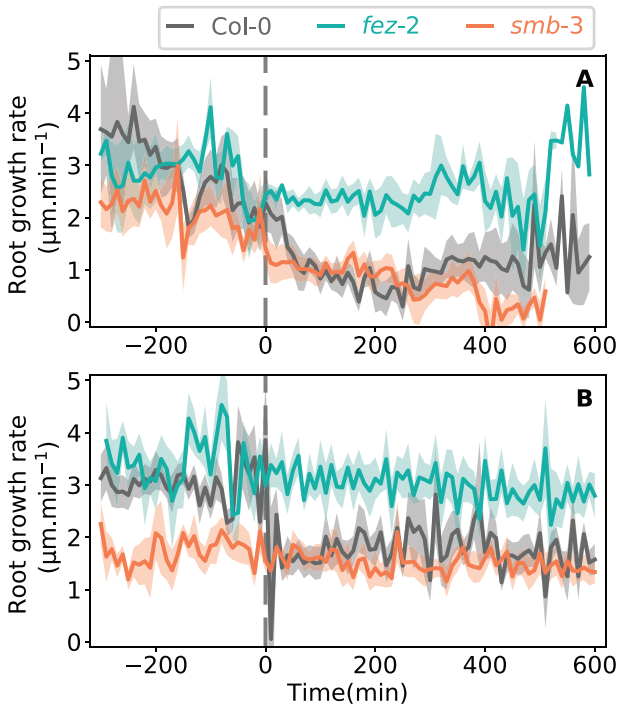

Fig. 10. Growth rate of Arabidopsis Col-0, *fez-2*, *smb-3* roots in two-layer media before and after contact with the interface. Growth rates are shown for roots that reorientated their growth after contact with the interface in (A) 0.2/0.3 % Phytagel medium and (B) 0.2/0.5 medium. Data are means (SD), 8<*n*<12. The dashed lines indicate the time of initial contact between the root tip and the interface.

Discussion

Our experimental design proved to be suitable for investigating root responses to differences in the strength of the growing medium. Precise characterization of mechanical properties of the media showed strong correlations between rigidity, penetration resistance, and Phytagel concentrations (Fig. 3). In addition, precise spatio-temporal analyses of root growth rate and root apex orientation allowed us to discriminate between the passive and active mechanisms involved in the reorientation. By using three genotypes of Arabidopsis with contrasting root-cap morphologies, namely the Col-0 wild-type and the mutants *fez-2* (pointed cap) and *smb-3* (rectangular-shaped cap), our study has resulted in a better understanding of the role of the root-cap structure in the responses to mechanical stresses.

Root apex reorientation involves both passive and active mechanisms

In our experimental system, roots grew first through a layer of medium of low strength before arriving at an interface with a layer of higher strength. In response to intermediate and high increases in strength at the interface, the growth rates of wild-type (WT) roots decreased significantly (Fig. 10, Supplementary Tables S3, S4). These decreases, which were observed for both penetrating and non-penetrating roots, were comparable to those observed in poplar roots confronted with a physical obstacle (Bizet *et al.*, 2016). This suggests the existence of a biological process that senses the increase in the strength of the medium and that subsequent responses were triggered in the WT roots (Bizet *et al.*, 2016).

Root growth against an interface in strength generates an increasing compression reaction force on the root (Kolb *et al.*, 2017). If the compression force reaches a critical value while the root is still in contact with the obstacle, buckling can occur as predicted by Euler's law (Bizet *et al.*, 2016). Buckling was observed for non-penetrating roots in all three genotypes and resulted in two distinct principal shapes being observed depending on the genotype and on the strength of the interface. When encountering an intermediate increase in in the strength of the medium, non-penetrating roots mostly developed a curly shape (Fig. 8A). This shape has previously been observed in *Medicago truncatula* roots growing in a two-layer Phytagel medium (Silverberg *et al.*, 2012) and, from a mathematical model based on the theory of buckling rods, it was attributed to a combination of helical buckling and simultaneous twisting near the root tip. For most of the curly roots, the first curvature was initiated in a zone between 400–700 μm from the tip of the root cap (Fig. 7). According to our kinematic analyses performed on roots growing in a

compliant single-layer medium, this seemed to correspond to the zone where the maximal elongation rate occurred (Fig. 5, Supplementary Fig. S2). Thus, the zone of curvature initiation may correspond to the zone of mechanical weakness described by Bizet *et al.* (2016). To confirm this, *in vivo* kinematic analyses would need to be carried out on roots growing in two-layer media. Taken together with previous studies, our results suggest that the curly shape is mainly driven by the mechanical response of the root acting as a 'growing' rod, the end of which is blocked by an obstacle.

The second distinct shape had a step-like appearance and was observed in roots mostly in response to the highest increase in the strength of the medium across the interface (Fig. 8B). In this case, the first curvature induced deviation of the root apex, which implied a change from axial to asymmetric radial forces being applied on the apex. The kinetics and the position of curvature initiation suggested that it may be interpreted as buckling. The first curvature was followed by the initiation of a second one, closer to the root apex, that allowed the root tip to regain a vertical position (Fig. 9). Since the second zone of curvature remained at a constant distance from the tip of the root cap after its establishment, it would have provided the root tip with a steady form from changing cells (Silk, 1992). The second curvature has previously been described as the result of the interaction between gravitropic and thigmotropic responses (Massa and Gilroy, 2003). The deviation of the root apex was preceded by a decrease in root growth rate that did not recover after relaxation of the axial mechanical stresses (Fig. 10). The initiation of the second curvature and the continuation of the reduced growth rate suggest that, even if the first curvature was initially provoked by buckling, the direction of the subsequent growth may have been reorientated in an active way.

The different patterns of the establishment of curvature suggest that the mechanical strength of the interface determines the subsequent root response (buckling or bending). An intermediate-strength interface may allow the root apex to sink into it, preventing its deviation after root buckling. In contrast, a strong interface seemed to be barely deformed by the root apex, which may then be free to deviate and may trigger active root reorientation.

The structure of the root cap affects the root response to an increase in the strength of the growth medium in the opposite way to that expected

Based on previous studies (Vollsnes *et al.*, 2010; Ruiz *et al.*, 2016; Colombi *et al.*, 2017*b*), we hypothesized that the shape of the root cap would influence the penetration ability of the root and its response to the strength of the medium by changing the distribution of mechanical stresses that result from the axially orientated external force. It has been suggested that a pointed root tip increases the axial stresses at the forefront of the tip rather than around it, resulting in enhanced initiation of cracks in the medium and enhanced penetration ability (Colombi *et al.*, 2017*b*). However, contrary to this hypothesis, roots of the *fez-2* mutant that have pointed tips (Fig. 4) exhibited reduced penetration abilities in the two-layer media compared to WT roots, whereas roots of *smb-3* that have dome-shaped tips exhibited enhanced penetration abilities. In the roots of the mutants, especially those of *fez-2*, given that the morphological alterations were mainly related to the structure of the cap, our results suggest that it is the cap structure that affects the establishment of the responses to the strength of the medium, but in a way that contradicted our hypothesis. This suggests either that the shape of the root cap is not the key feature that determines the root responses, or that another factor could influence the establishment of the responses. In light of this, attention should be paid to the relative cap rigidity of the WT and mutant roots. The loss or accumulation of root-cap cell layers, modulating its dimensions, could modify the local bending rigidity and compression behaviour that drive the ability of root apex to go forward in the medium. In *fez-2* roots, the potential benefit of a more pointed cap shape with regards to penetration ability could be reduced by low cap rigidity, meaning that the root could not experience high mechanical stress without undergoing buckling or compressive rupture.

The differences in penetration abilities between the mutant and WT roots may be attributable to their different critical buckling forces. Our results showed that the *fez-2* roots applied a lower critical axial force on the interface before buckling compared with the WT whilst the *smb-3* roots applied a higher critical force (Fig. 6). These differences may be explained either by differences in diameter and/or rigidity at the buckling zone of the root, or by differences in the length of the growth zone, as defined by Euler's law. Our characterizations of the root morphologies of the mutants did not reveal any differences in the diameter or length of the growth zone compared to the WT roots in conditions where the strength of the medium was low (Fig. 4)-. Our results suggest that either the rigidity of mutant roots was different compared to that of the WT, or that the length of the growth zone, tissue rigidity, and/or root diameter may have been modulated differently between the genotypes in response to an increase in the strength of the medium.

Further experiments need to be conducted to confirm either of these hypotheses, such as atomic force microscopy assays in order to accurately characterize local rigidity in the root tissues. In particular, the lower and higher root diameters at the quiescent centre, resulting from fewer and more lateral root-cap cell layers flanking the *fez-2* and *smb-3* root apexes, respectively, could constitute an advantage for penetrating harder layers in the medium by affecting local rigidity in the roots (Bennett *et al.*, 2010; Fendrych *et al.*, 2014). In addition, *in vivo* kinematic analyses could be performed on roots growing in two-layer media in order to define the effect of the increase in strength on the length of the growth zone. At present, if the second hypothesis turns out to be true, we may speculate that increases in the strength of the medium are perceived by root-cap cells and that signal transduction triggers responses in the elongation zone. In *fez-2* roots, the reduction in the number of cell layers in the cap may alter the mechanosensitivity and thus affect the establishment of root responses to an increase in the strength of the medium. The fact that the growth rate of *fez-2* roots was not affected by the strength of the medium supports this hypothesis. A properly formed root cap may be required to trigger the signal perception and transduction processes and

thus to allow the root to respond to an increase in the strength of the medium.

Conclusions

During their progression in soil, roots frequently face physical heterogeneities that they must either move or cross by generating mechanical forces, or must circumvent by reorientating their growth. Our study provides new insights into the role of the root cap in root penetration and reorientation in response to variations in the strength of the growth medium. When Arabidopsis primary roots encounter layers in the medium with increasing strength, they adopt three main types of response: root penetration, root buckling without apex deviation that leads to a curly shape, or root buckling followed by apex deviation that leads to a step-like shape. These responses were different in the roots of the *fez-2* and *smb-3* mutants, which possess more pointed and more rectangular cap shapes, respectively. The differences in penetration ability, reduced in *fez-2* roots and enhanced in *smb-3* roots, seems to result from different resistances to root buckling. These results suggest that the structure of the cap could affect root responses to the strength of the growth medium by influencing root resistance to buckling.

Supplementary data

Supplementary data are available at *JXB* online.

Fig. S1. Images of the two-layer Phytagel media that were used to study root responses.

Fig. S2. Cell length and velocity profiles of roots growing in a single-layer medium.

Fig. S3. Gravitropic responses of roots growing in a single-layer medium.

Fig. S4. Diameter of the roots at 500 μm from the tip of the root cap when grown in a single-layer medium.

Table S1. Characteristics of the zones of curvature formed in reorientating roots in the 0.2/0.3 medium.

Table S2. Characteristics of the zones of curvature formed in reorientating roots in the 0.2/0.5 medium.

Table S3. Detailed growth rates of penetrating roots in the 0.2/0.2 and 0.2/0.3 media.

Table S4. Detailed growth rates of reorientating roots in the 0.2/03 and 0.2/0.5 media.

Video S1. Time-lapse movie of a reorientating wild-type root in the 0.2/0.3 medium.

Video S2. Time-lapse movie of a reorientating *smb-3* root in the 0.2/0.3 medium.

Video S3. Time-lapse movie of a reorientating *fez-2* root in the 0.2/0.3 medium.

Video S4. Time-lapse movie of a reorientating wild-type root in the 0.2/0.5 medium.

Video S5. Time-lapse movie of a reorientating *fez-2* root in the 0.2/0.5 medium.

Video S6. Time-lapse movie of a reorientating *smb-3* root in the 0.2/0.5 medium forming a step-like shape.

Video S7. Time-lapse movie of a reorientating *smb-3* root in the 0.2/0.5 medium forming a wavy shape.

Acknowledgements

We would like to thank Ben Scheres and Viola Willemsen (University of Utrecht, The Netherlands) for donating the mutant lines. We thank Evelyne Kolb and Marie-Bogeat-Triboulot for fruitful discussion. This research received financial support from the French Space Agency (CNES) and INRA programs. JR received a doctoral grant from the French National Ministry of Education and Research. HC received a Postdoctoral grant from the Auvergne-Rhône Alpes Council with co-funding from FEDER. FB received a Postdoctoral grant from the CNES.

References

Ahearne M, Yang Y, El Haj AJ, Then KY, Liu KK. 2005. Characterizing the viscoelastic properties of thin hydrogel-based constructs for tissue engineering applications. Journal of the Royal Society, Interface **2**, 455–463.

Arnaud C, Bonnot C, Desnos T, Nussaume L. 2010. The root cap at the forefront. Comptes Rendus Biologies **333**, 335–343.

Barlow PW. 2003. The root cap: cell dynamics, cell differentiation and cap function. Journal of Plant Growth Regulation **21**, 261–286.

Bengough AG, Hans J, Bransby MF, Valentine TA. 2010. PIV as a method for quantifying root cell growth and particle displacement in confocal images. Microscopy Research and Technique **73**, 27–36.

Bennett T, Sanchez-perez GF, Campilho A, Willemsen V, Snel B, Scheres B. 2010. SOMBRERO, BEARSKIN1, and BEARSKIN2 regulate root cap maturation in Arabidopsis. The Plant Cell **22**, 640–654.

Bennett T, van den Toorn A, Willemsen V, Scheres B. 2014. Precise control of plant stem cell activity through parallel regulatory inputs. Development **141**, 4055–4064.

Bizet F, Bengough AG, Hummel I, Bogeat-Triboulot MB, Dupuy LX. 2016. 3D deformation field in growing plant roots reveals both mechanical and biological responses to axial mechanical forces. Journal of Experimental Botany **67**, 5605–5614.

Chauvet H, Pouliquen O, Forterre Y, Legué V, Moulia B. 2016. Inclination not force is sensed by plants during shoot gravitropism. Scientific Reports **6**, 35431.

Colombi T, Braun S, Keller T, Walter A. 2017*a*. Artificial macropores attract crop roots and enhance plant productivity on compacted soils. The Science of the Total Environment **574**, 1283–1293.

Colombi T, Kirchgessner N, Walter A, Keller T. 2017*b*. Root tip shape governs root elongation rate under increased soil strength. Plant Physiology **174**, 2289–2301.

Fendrych M, Van Hautegem T, Van Durme M, *et al*. 2014. Programmed cell death controlled by ANAC033/SOMBRERO determines root cap organ size in Arabidopsis. Current Biology **24**, 931–940.

Hanaor DAH, Gan Y, Einav I. 2015. Contact mechanics of fractal surfaces by spline assisted discretisation. International Journal of Solids and Structures **59**, 121–131.

Huysmans M, Buono RA, Skorzinski N, Radio MC, De Winter F, Parizot B, Mertens J, Karimi M, Fendrych M, Nowack MK. 2018. NAC transcription factors ANAC087 and ANAC046 control distinct aspects of programmed cell death in the Arabidopsis columella and lateral root cap. The Plant Cell **30**, 2197–2213.

Iijima M, Barlow PW, Bengough AG. 2003*a*. Root cap structure and cell production rates of maize (*Zea mays*) roots in compacted sand. New Phytologist **160**, 127–134.

Iijima M, Higuchi T, Barlow PW, Bengough AG. 2003*b*. Root cap removal increases root penetration resistance in maize (*Zea mays* L). Journal of Experimental Botany **54**, 2105–2109.

Jin K, Shen J, Ashton RW, Dodd IC, Parry MA, Whalley WR. 2013. How do roots elongate in a structured soil? Journal of Experimental Botany **64**, 4761–4777.

Kolb E, Legué V, Bogeat-Triboulot MB. 2017. Physical root–soil interactions. Physical Biology **14**, 065004.

Kumpf RP, Nowack MK. 2015. The root cap: a short story of life and death. Journal of Experimental Botany **66**, 5651–5662.

Liu Y, Lai N, Gao K, Chen F, Yuan L, Mi G. 2013. Ammonium inhibits primary root growth by reducing the length of meristem and elongation zone

and decreasing elemental expansion rate in the root apex in *Arabidopsis thaliana*. PLoS ONE **8**, 1–11.

Massa GD, Gilroy S. 2003. Touch modulates gravity sensing to regulate the growth of primary roots of Arabidopsis thaliana. The Plant Journal **33**, 435–445.

Materechera SA, Alston AM, Kirby JM, Dexter AR. 1992. Influence of root diameter on the penetration of seminal roots into a compacted subsoil. Plant and Soil **144**, 297–303.

Ruiz S, Straub I, Schymanski SJ. 2016. Experimental evaluation of earthworm and plant root soil penetration – cavity expansion models using cone penetrometer analogs. Vadose Zone Journal **15**, vzj2015.09.0126.

Sato EM, Hijazi H, Bennett MJ, Vissenberg K, Swarup R. 2015. New insights into root gravitropic signalling. Journal of Experimental Botany **66**, 2155–2165.

Schiavi A, Cuccaro R, Troia A. 2016. Strain-rate and temperature dependent material properties of Agar and Gellan Gum used in biomedical applications. Journal of the Mechanical Behavior of Biomedical Materials **53**, 119–130.

Schneider CA, Rasband WS, Eliceiri KW. 2017. NIH image to ImageJ: 25 years of image analysis. Nature Methods **9**, 671–675.

Silk WK. 1992. Steady form from changing cells. International Journal of Plant Science **153**, 49–58.

Silk WK, Erickson RO. 1979. Kinematics of plant growth. Journal of Theoretical Biology **76**, 481–501.

Silverberg JL, Noar RD, Packer MS, Harrison MJ, Henley CL, Cohen I, Gerbode SJ. 2012. 3D imaging and mechanical modeling of helical buckling in *Medicago truncatula* plant roots. Proceedings of the National Academy of Sciences, USA **109**, 16794–16799.

Timoshenko SP, Goodier JN. 1970. Theory of elasticity. New York: McGraw-Hill.

Vicré M, Santaella C, Blanchet S, Gateau A, Driouich A. 2005. Root border-like cells of Arabidopsis. Microscopical characterization and role in the interaction with rhizobacteria. Plant Physiology **138**, 998–1008.

Vollsnes AV, Futsaether CM, Bengough AG. 2010. Quantifying rhizosphere particle movement around mutant maize roots using time-lapse imaging and particle image velocimetry. European Journal of Soil Science **61**, 926–939.

Willemsen V, Bauch M, Bennett T, Campilho A, Wolkenfelt H, Xu J, Haseloff J, Scheres B. 2008. The NAC domain transcription factors FEZ and SOMBRERO control the orientation of cell division plane in Arabidopsis root stem cells. Developmental Cell **15**, 913–922.

Yamamoto C, Sakata Y, Taji T, Baba T, Tanaka S. 2008. Unique ethylene-regulated touch responses of *Arabidopsis thaliana* roots to physical hardness. Journal of Plant Research **121**, 509–519.

Yan J, Wang B, Zhou Y. 2017. A root penetration model of *Arabidopsis thaliana* in phytagel medium with different strength. Journal of Plant Research **130**, 941–950.